Available online at www.sciencedirect.com
ScienceDirect
Polymer 49 (2008) 412–421
polymer
www.elsevier.com/locate/polymer

Direct photobleaching of acrylates in polymethylsilsesquioxane films by 193 nm irradiation

Carlos N. Sanrame [a], Yujian You [b], Mike Talley [b], Marius G. Ivan [a], J.C. Scaiano [a,*]

[a] Department of Chemistry, University of Ottawa, 10 Marie Curie, Ottawa, ON K1N 6N5, Canada
[b] Rohm and Haas Company, Emerging Technologies, 727 Norristown Road, Spring House, PA 19474-0904, USA

Received 12 June 2007; received in revised form 14 November 2007; accepted 17 November 2007
Available online 27 December 2007

Abstract

The direct irradiation of trimethylolpropane propoxylate triacrylate (PPO-TMPTA) – a good chromophore at 193 nm – in thin films of polymethylsilsesquioxanes (PMSSQs), leads to efficient photobleaching at that wavelength with high contrast. The photobleaching is due to loss of the acrylate vinyl C=C bond, as confirmed by FTIR and NMR. Other chromophores, such as non-conjugated dienes and dialkyldiazenes, were evaluated and the photobleaching was found to be less efficient compared to acrylates. We analyzed the effect of the film composition (matrix, acrylate, photoinitiator and plasticizers) as well as the processing atmosphere on the final contrast and speed of the photobleaching. The PMSSQ matrix was superior to polyacrylates and the best results were obtained with acrylates containing long flexible arms such as PPO-TMPTA. The addition of radical photoinitiators increases slightly the photobleaching speed, but not as much as addition of plasticizers. The presence of oxygen slows down the process without stopping it. A mechanism is proposed in which the acrylate triplet state can add or couple to other acrylates, generating 1,4-diradicals. Alternatively photoionization can also trigger a cascade of events leading to C=C loss.

Keywords: Contrast agent; Acrylates; Laser photolysis

1. Introduction

Acrylate-based monomers, crosslinkers and oligomers, have found widespread use in technological applications, including as components of ultraviolet (UV) photocurable and photopolymerizable coatings, adhesives and inks. In these photoactive formulations, there are typically two reactive components with well-defined roles, a small amount of a photoinitiator and an acrylate. The photoinitiator absorbs UV light and generates radicals, which add to an acrylate, initiating polymerization; new applications and improved formulations are emerging regularly [1–6]. Recently, the direct 222 nm photopolymerization of neat acrylates in thin films in the absence of photoinitiators was proposed as an alternative to the use of photoinitiators and facilitated by the commercialization of deep UV (DUV) excimer lamps [1,7–9]. Direct DUV excitation of the acrylate generates species that lead to polymerization or crosslinking.

During the photopolymerization of acrylates, the α,β unsaturated carbonyl chromophores are converted to alkyl carbonyls resulting in photobleaching. Thus, three properties of acrylates make them suitable for use as DUV photobleachable materials: high absorbance, photoreactivity, and a 'transparent' photoproduct.

Photochromic and photobleachable materials have widespread applications [10,11]. In particular, some photobleachable systems have been used in contrast enhanced photolithography to improve photoresist performance in the fabrication of computer chips. The use of contrast enhancement layers (CELs) and materials (CEM) to improve and extend the resolution of resist systems was demonstrated by West and Griffing in the early 1980s [12–14]. The key component of a CEL is the photobleaching chromophore. Photobleachable or photochromic systems are well known,

* Corresponding author. Fax: +1 613 562 5633.
E-mail address: tito@photo.chem.uottawa.ca (J.C. Scaiano).

0032-3861/$ - see front matter © 2007 Elsevier Ltd. All rights reserved.
doi:10.1016/j.polymer.2007.11.045

particularly in the UV–vis range. Some of the well studied systems include diazene/azide, spiropyrane and *cis–trans* isomerizations [10]. However, the photoproducts of the common photobleachable materials are rarely 'transparent' at wavelengths below 250 nm. Acrylic materials are promising candidates for high contrast photobleachable systems at DUV wavelengths due to their optical characteristics, photoreactivity, and their relatively simple and transparent photoproducts. We undertook the detailed study of acrylate photobleaching at 193 nm because of their potential lithographic CEM applications. During the course of our study, several other chromophores were considered, such as non-conjugated dienes and dialkyl diazenes. Preliminary results with these chromophores indicated that a high contrast and a low residual absorbance were more difficult to achieve after 193 nm irradiation of diene and dialkyldiazene systems than in acrylates.

This work focuses on the 193 nm photobleaching of PMSSQ films containing acrylates, materials that could be used in CEL or CEM applications. PMSSQ is a convenient matrix because acrylic monomers or crosslinkers are usually liquids and less likely to yield good thin films by spin coating. PMSSQ, which is very transparent at 193 nm, improves the mechanical properties of the blend and can form quality films by spin coating, facilitating the incorporation of additives in order to increase the photobleaching efficiency. The effects of several variables, such as the film composition (matrix, acrylate, photoinitiator, plasticizers), as well as the processing environment, on the final contrast and speed of photobleaching were analyzed. In addition, FTIR and NMR were used to examine the process. We note that photobleaching is normally accompanied by an increase in the toughness of the film, even in the absence of photoinitiators, particularly when acrylic crosslinkers are used.

2. Experimental

2.1. Materials

Relevant formulas are given in Scheme 1. The following chemicals were purchased from Aldrich and used as-received, unless specified otherwise: trimethylolpropane triacrylate (TMPTA), 2-butanone (MEK), propylene glycol methyl ether acetate (PGMEA), 1,4,4α,8α-tetrahydro-*endo*-1,4-methanonaphthalene-5,8-dione (THMND), dicyclopentadiene (DCPD), 5-vinyl-2-norbornene (VNB), 2,2′-azobis(2-methylpropionitrile) (AIBN), 1,1′-azobis-(cyclohexanecarbonitrile) (ACHN),

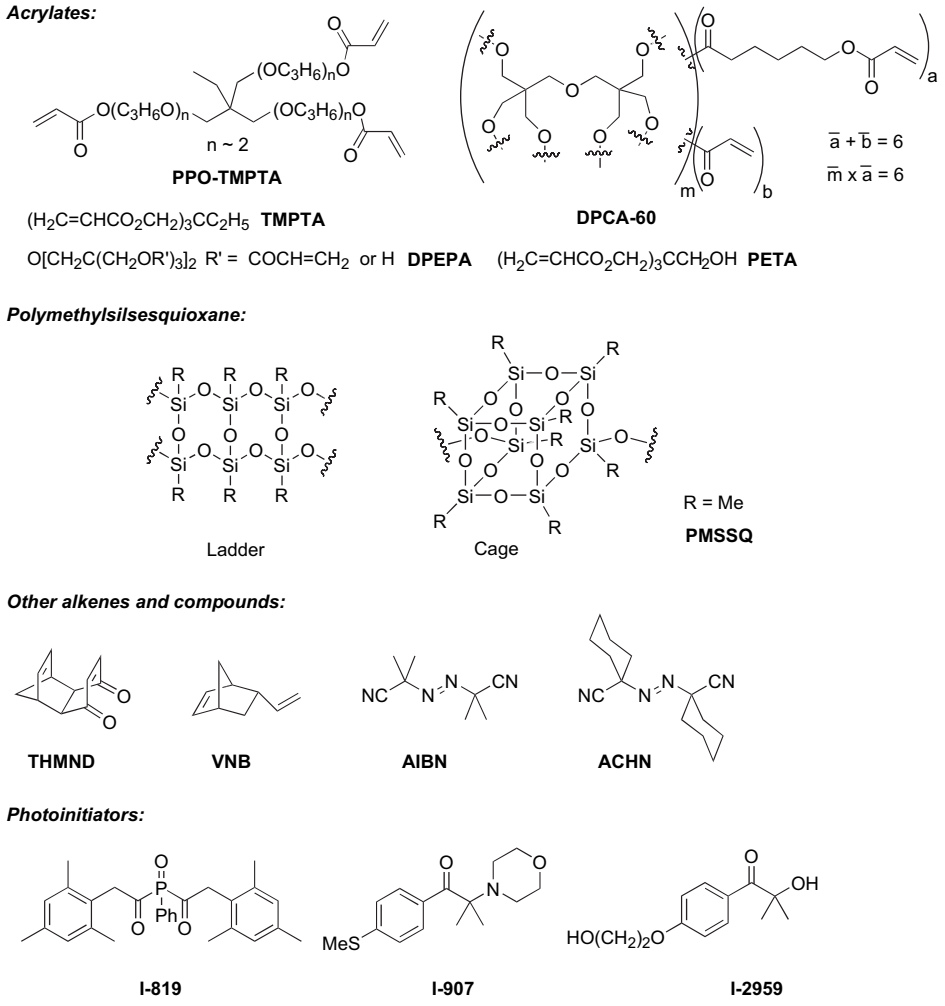

Scheme 1.

trimethylolpropane propoxylate triacrylate, $M_n \sim 644$ (PPO-TMPTA), pentaerythritol triacrylate (PETA), dipentaerythritol pentaacrylate (DPEPA) and phenyl bis(2,4,6-trimethylbenzoyl)phosphine oxide (I-819). Caprolactone modified dipentaerythritol hexaacrylate (DPCA-60) was obtained from Sartomer company. 2-Methyl-4′-(methylthio)-2-morpholinopropiophenone (I-907) and 2-hydroxy-4′-(2-hydroxyethoxy)-2-methylpropiophenone (I-2959) were obtained from Ciba Specialty Chemicals.

Polymethylsilsesquioxane (PMSSQ) was purchased from Technical Glass Products and stored at about 4 °C. PS071 is a dimethylsiloxane–ethylene oxide copolymer obtained from the United Chemical Technologies. The copolymers MMA (methyl methacrylate)/TMPTA, BMA(butyl methacrylate)/TMPTA, and BA(butyl acrylate)/TMPTA were synthesized according to the literature [15]. The acrylic nanoparticles, abbreviated as NP1, NP2 and NP3 and used as plasticizers, were synthesized by a reported method [15] with the following composition: NP1, MeO–PEO–MA/PDMA (90/10), NP2, HO–PPO–MA/EDMA (90/10), NP3, PPGMEA260/TMPTA (9010). The acrylates, poly(ethylene glycol) methyl ether methacrylate (MeO–PEO–MA), poly(propylene glycol) methacrylate (HO–PPO–MA), poly(propylene glycol) methyl ether acrylate (PPGMEA260), propylene glycol dimethacrylate (PDMA), ethylene glycol dimethacrylate (EDMA), and trimethylolpropane triacrylate (TMPTA), used for the synthesis of the nanoparticles, were obtained from Aldrich.

2.2. Techniques

Irradiations at 193 nm were conducted with a Lambda Physik (Compex 110) or GSI Lumonics (PM846) laser operated at 1–20 Hz. For the Lumonics laser the power was measured using a power head Coherent (J45LP-MB), with a voltage response of 16.1 VJ^{-1} at 1064 nm connected to a Molectron joulemeter ratiometer (JD2000). UV–vis spectra were recorded on a Hewlett Packard HP-8453 or HP-8251 spectrometer. The film thickness was measured by interferometry using a Luzchem TFA-11 thin film analyzer or a Dektak(3)-30 surface profiler.

The atomic force microscopic (AFM) measurements were carried out with a D5000 scanning probe microscope using an RTESP tip (Veeco Instruments). The AFM images were obtained (2×2 and 10×10 μm) in phase and topographic modes. The samples were conditioned in a desiccator with a salt bath so that a 55% relative humidity was maintained before they were moved to the D5000 scanning probe microscope and imaged.

FTIR spectra were obtained with a Thermo Nicolet model Nexus 670 spectrometer. ^1H (500 MHz) and ^{13}C (125 MHz) NMR spectra were obtained with a Bruker Avance 500 and the chemical shifts are referred to tetramethylsilane.

2.3. Procedure for the evaluation of photobleaching

A typical evaluation of the chromophore photobleaching characteristics involved the following steps: (1) formulation of all components in a compatible solution using MEK or PGMEA as solvent. Typically the solids content was ~20%, and the dry weight ratio of matrix to chromophore was about 9:1; (2) spin coating of the solution on 1″ or 2″-fused silica discs, followed by 1 min baking at 90 °C. This step was omitted when the sample contained thermolabile components, such as azo compounds; (3) measurement of the transmittance before exposure; (4) laser irradiation at 193 nm. Exposure time was adjusted to provide the desired energy dose; (5) measurement of the transmittance after exposure; (6) plot transmittance against energy dose (*E*-dose) and fitting of the linear portion of the plot to obtain the slope ($\Delta T\%/E$-dose ($mJ\,cm^{-2}$)). These plots were used to compare several parameters to rationalize the best case for the higher transmittance at the end point, the minimum energy dose to get to this point, and the bleaching rate (the slope from the plot). Direct comparison of slopes is reasonable provided that the initial transmittances are similar.

3. Results and discussion

Fig. 1 shows the absorption spectra for a film containing PPO-TMPTA in PMSSQ before and after 193 nm excimer laser exposure to 2.0 $J\,cm^{-2}$. During irradiation the high absorbance film is rendered practically transparent at wavelengths above 190 nm. This composition outperforms many other formulations tested; thus under similar conditions films of PMSSQ, each containing dienes or dialkyl diazenes (THMND, DCPD, VNB, AIBN or ACHN) as radical generators showed that at the end point the absorbance was one-half or more of the initial absorbance, as shown in Fig. 2.

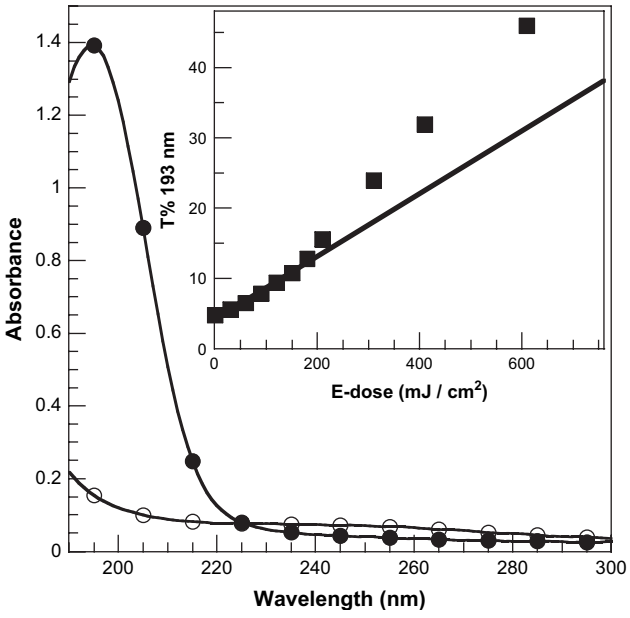

Fig. 1. Absorption spectra of a PMSSQ film containing PPO-TMPTA before (solid circles) and after (open circles) exposure to 2.0 $J\,cm^{-2}$ at 193 nm. Inset: film transmittance at 193 nm, plotted against incident energy dose. The slope is obtained by least square regression of the linear portion of the plot and is representative of the initial photobleaching rate.

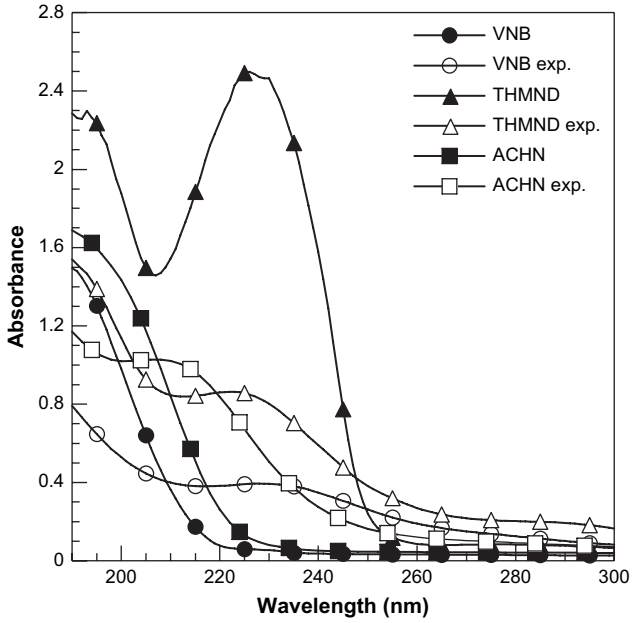

Fig. 2. Absorption spectra of PMSSQ films containing 10% of THMND (triangles), VNB (circles) or ACHN (squares) before (solid symbols) and after (open symbols) 193 nm exposure to a 2.0 J cm^{-2} dose.

The lack of a good contrast for these chromophores turned our attention to the efficient bleaching of the acrylates.

The inset in Fig. 1 shows the bleaching curve for 193 nm exposure. The initial steep slope was used as a measure of the bleaching rate. The promising result obtained for PPO-TMPTA in PMSSQs (Fig. 1) led us to explore the effect of film composition (matrix, acrylate, photoinitiator, plasticizers) as well as processing environment on the final contrast and speed of the photobleaching. The results are detailed in the following sections.

3.1. Matrices

Matrix materials provide mechanical support as binders for the acrylates and should not be involved in the photochemical reactions and should be optically transparent at the exposure wavelength, with good film-forming properties; for CEL (rather than CEM) applications compatibility with other layers and their casting solvents is also required. PMSSQ was selected as the matrix for most of our studies due to its transparency at 193 nm; even a 20 μm PMSSQ film has only 0.05 absorbance, decreasing to 0.02 after exposure to 2.0 J cm^{-2} at 193 nm. Mixtures of PMSSQ, acrylates and additives were spin coated from MEK or PGMEA, to form good films. The film thickness was adjusted by changing the solvent content of the mixture or the spinning rate.

The structure, functional groups, and glass transition temperature (T_g) of the matrix material may play an important role in the photobleaching process. As shown in Table 1, PMSSQ (entry 5) appeared to be the best matrix, allowing faster bleaching in comparison with the acrylic copolymers (entries 1–4). In these experiments a small amount of radical photoinitiator (I-819) was added to increase the rate of photobleaching (see below). PMSSQ with no apparent T_g, but with continuous drop in viscosity between room temperature and 150 °C, starts to cure by a condensation reaction at temperatures above 150–180 °C. We have observed that acrylic matrices are not ideal because the photobleaching process is slow, and they are prone to photoreact on 193 nm irradiation, with an increase in the absorbance at the irradiation wavelength, as already reported for PMMA [16].

Matrix materials must be compatible with the chromophore and other film components. Phase separation into large domains can cause problems due to light scattering and surface irregularities. Fig. 3 shows the AFM images, at scan sizes of 2 and 0.5 μm, of films containing (A) only PMSSQ, (B) TMPTA in PMSSQ, and (C) PPO-TMPTA in PMSSQ. The plot for the film containing TMPTA (Fig. 3B) shows spherically shaped droplets of different sizes, 5–50 nm, some of them protruding from the surface. In contrast, the film containing PPO-TMPTA does not show the presence of large size agglomeration at the level of resolution examined, but some small uniform droplets (5–12 nm) (Fig. 3C) and looks almost identical to the PMSSQ film (Fig. 3A). Consequently, the formation of microdomains of TMPTA in PMSSQ indicates phase separation and low mutual compatibility. On the other hand, PPO-TMPTA shows better compatibility with PMSSQ.

Table 1
Photobleaching of films containing PPO-TMPTA (10 wt%)[a] under several conditions

Entry	Matrix	Env.	Initiator	Wt%	T% Initial	T% Final	E-dose[b] mJ cm^{-2}	Bleaching rate (ΔT%/E-dose)
1	MMA/TMPTA[c]	N_2	I-819	0.37	0.55	2.70	500	0.04
2	BMA/TMPTA[c]	N_2	I-819	0.25	2.02	4.56	500	0.05
3	BA/TMPTA[c]	N_2	I-819	0.20	0.16	0.75	500	0.06
4	BA/TMPTA[c]	N_2	I-819	0.26	18.3	22.0	500	0.07
5	PMSSQ	N_2	I-819	0.28	11.1	56.6	500	0.9
6	PMSSQ	N_2			13.5	63.2	500	1
7	PMSSQ	Vacuum			14.5	66.4	500	1.2
8	PMSSQ	Air	I-2959	0.02	18.20	>58.8	>300	1.4
9	PMSSQ	N_2	I-907	0.01	18.24	>58.59	>300	1.4
10	PMSSQ	N_2	I-819	0.10	15.13	>70.1	>500	1.2
11	PMSSQ	N_2	I-819	0.01	16.2	69.2	>400	1.4
12	PMSSQ	N_2			4.7	>46	>610	0.8

[a] The solvent used for mixing and spin coating was PGMEA.
[b] Irradiation at a repetition rate of 20 Hz, 5.0 mJ cm^{-2} pulse^{-1}.
[c] In the copolymer the content of TMPTA is 10%.

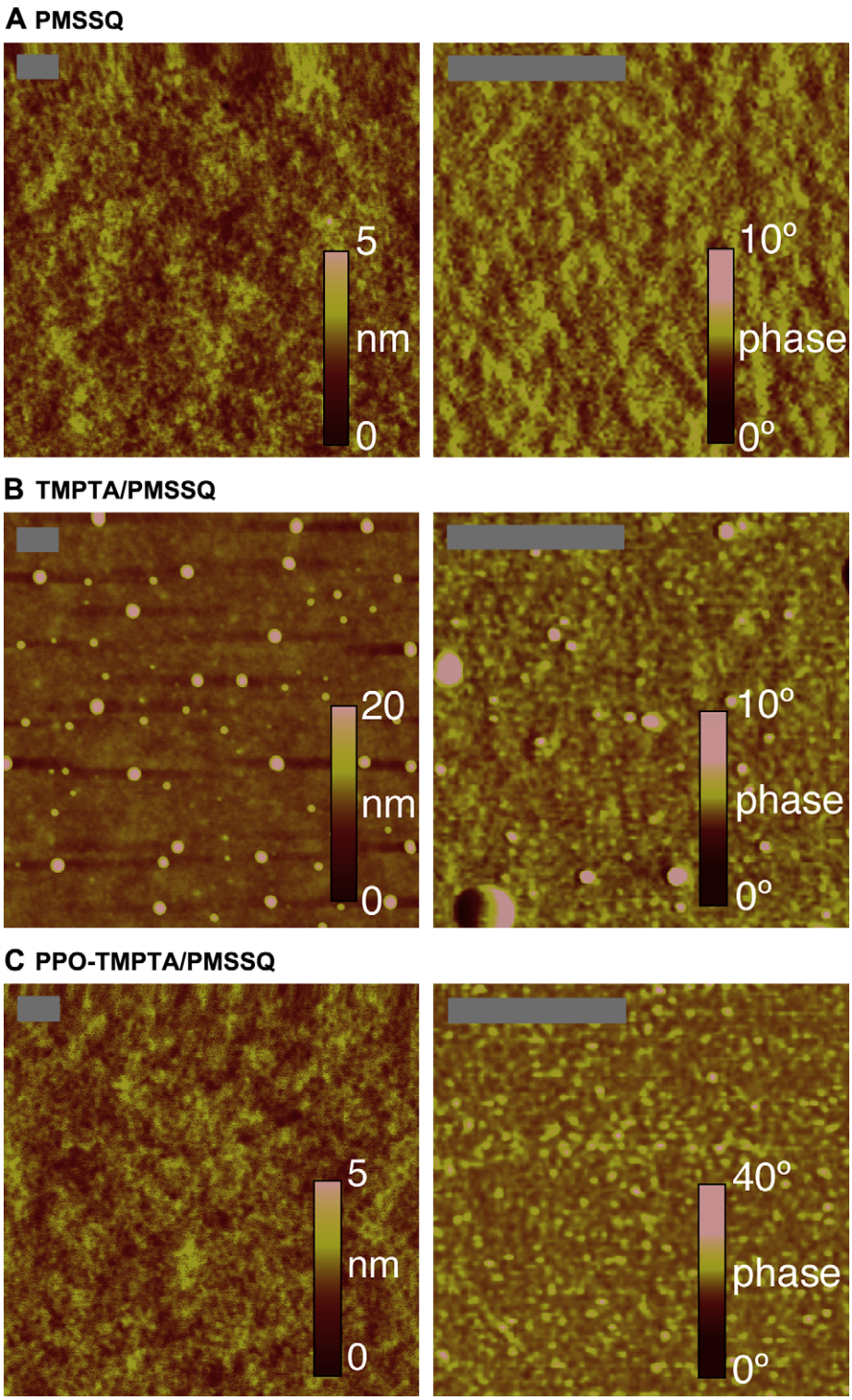

Fig. 3. AFM images of (A) PMSSQ, (B) TMPTA/PMSSQ, and (C) PPO-TMPTMA/PMSSQ thin films. All were subjected to thermal treatment at 120–150 °C for ~3 h. Panels on the left are based on height and on the right are based on phases. The gray bar length is 200 nm.

3.2. Processing environment

Oxygen reacts with radicals that can form upon irradiation, interfering with the propagation of radical chain reactions. We have examined the oxygen effect on the photobleaching of films containing PPO-TMPTA in PMSSQ with small amounts of the photoinitiator I-819. The photobleaching rates were measured under air, nitrogen and vacuum (Table 1, entries 6–8). The bleaching rate decreases slightly under nitrogen and vacuum compared to air.

3.3. Initiators

Several photoinitiators were tested in films (Scheme 1), and their influence on the rate of photobleaching of PPO-TMPTA were determined. Entries 8–11 in Table 1 correspond to samples containing photoinitiators I-2959, I-907 and I-819, at low and high load; entry 12 corresponds to the sample without photoinitiator and was used as a control. The photobleaching rates indicate that radical photoinitiators at loads ~0.01 to 0.02% increase the rate of photobleaching and that this rate is hardly influenced by the photoinitiator's structure. On the other hand, a 10-fold increase in the load of I-819 yields a lower bleaching rate, yet still higher than that without photoinitiator. Thus, small amounts of photoinitiator can be used to increase the photobleaching efficiency; however, under our experimental conditions, their effect is small and their presence is not required for photobleaching to occur.

3.4. Acrylates

The acrylates studied in this work are common cross-linkers; they have different numbers of acrylate moieties per molecule, and different 'arm' lengths (Scheme 1). They were selected to allow the evaluation of how the number and density of reactive units per molecule, as well as molecular flexibility, influence the photobleaching rate. Further, the different structures and compositions of the monomers can affect their compatibility with the PMSSQ matrix. TMPTA, PETA and DPEPA have 3, 3, and 5/6 acrylate units per molecule, respectively, and the molecular backbone for these compounds is similar and rather inflexible. In contrast, PPO-TMPTA and DPCA-60, which contain PPO and caprolactone units on the backbone, are more flexible. The photobleaching rates for the acrylates in PMSSQ are reported in Table 2. The bleaching rates were very low, including the control of PPO-TMPTA; however, TMPTA, PETA and DPEPA show much lower rates compared to those of PPO-TMPTA and DPCA-60. A high density of functional groups per molecule does not make the process faster as shown by comparing DPEPA and PPO-TMPTA. The results indicate that faster photobleaching occurs when the acrylates have a flexible backbone allowing functional groups to adopt the conformations preferred for reaction as well as increase the compatibility with the PMSSQ matrix.

Table 2
Photobleaching of PMSSQ films containing the photoinitiator I-819 (0.12%) and different monomers (10 wt%)

Entry	Monomer	*T*% Initial	*T*% Final	*E*-dose[a] mJ cm^{-2}	Bleaching rate ($\Delta T\%/E$-dose)
1	PPO-TMPTA	0.29	1.37	400	0.04
2	TMPTA	0.27	0.24	400	−0.002
3	PETA	0.23	0.24	400	0
4	DPEPA	0.24	0.26	400	0.0004
5	DPCA-60	0.28	1.44	400	0.05

[a] The irradiation was done at a repetition rate of 20 Hz, 5 mJ cm^{-2} pulse^{-1}.

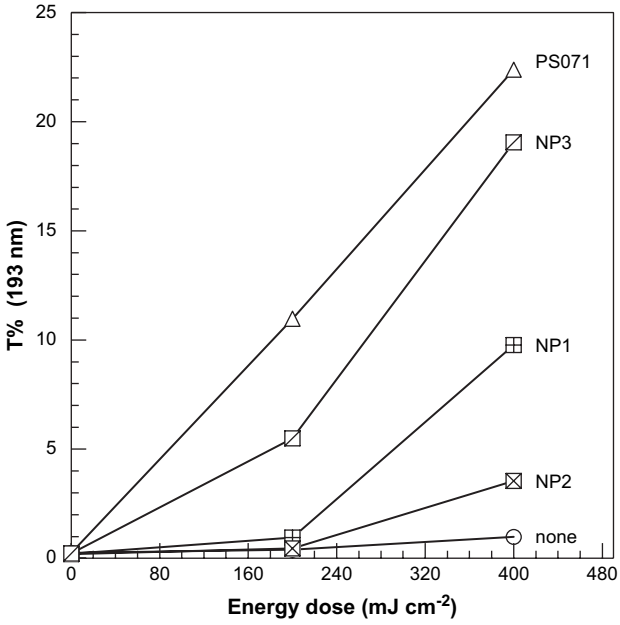

Fig. 4. Transmittance plots for PPO-TMPTA/PMSSQ thin films containing different plasticizers after 193 nm exposure. NP are nanoparticles of acrylates/(ethoxy)propoxyacrylate copolymers (see text for details), PS071 is a dimethylsiloxane–ethylene oxide copolymer with a viscosity of 20 cP at room temperature. The films consisted of PMSSQ, plasticizers (30 wt% where it applies), 10 wt% of PPO-TMPTA, and photoinitiator I-819 at 1–2% loading based on the amount of PPO-TMPTA.

3.5. Plasticizers

Some low glass transition temperature (T_g) plasticizers were added to facilitate the diffusion of reactive species in the matrix. They were chosen due to their compatibility with the matrix; their addition greatly increases the rate of PPO-TMPTA photobleaching, as shown in Fig. 4. The best improvement was obtained using dimethylsiloxane–ethylene oxide copolymers, in particular PS071. We also attempted to use acrylic nanoparticles [15]; however, the increase was not as significant as in the case of PS071. The presence of these plasticizers increased the absorbance of the film, and even though the photobleaching of these plasticizers alone was not tested, it is expected to be insignificant compared to that of PPO-TMPTA.

3.6. FTIR studies

Infrared spectroscopy proved valuable for monitoring changes in functional groups [17] upon irradiation. Thin films, 700 nm thick, of PPO-TMPTA in PMSSQ were deposited on NaCl windows by spin coating (2000 rpm) a solution of PPO-TMPTA/PMSSQ 15:85 wt% in MEK followed by 90 °C baking for 6 min. Their IR and the UV–vis spectra were recorded before and after successive 193 nm irradiation steps. The irradiation was stopped when further irradiation led to no more changes in the UV–vis and FTIR spectra, thus reaching the 'photobleaching end point'. Fig. 5 shows the FTIR spectra recorded before and at the end point. Most of the IR bands in the unexposed sample can be readily assigned to the acrylate [17,18] or to PMSSQ [17,19], as indicated by asterisks and crosses in the figure.

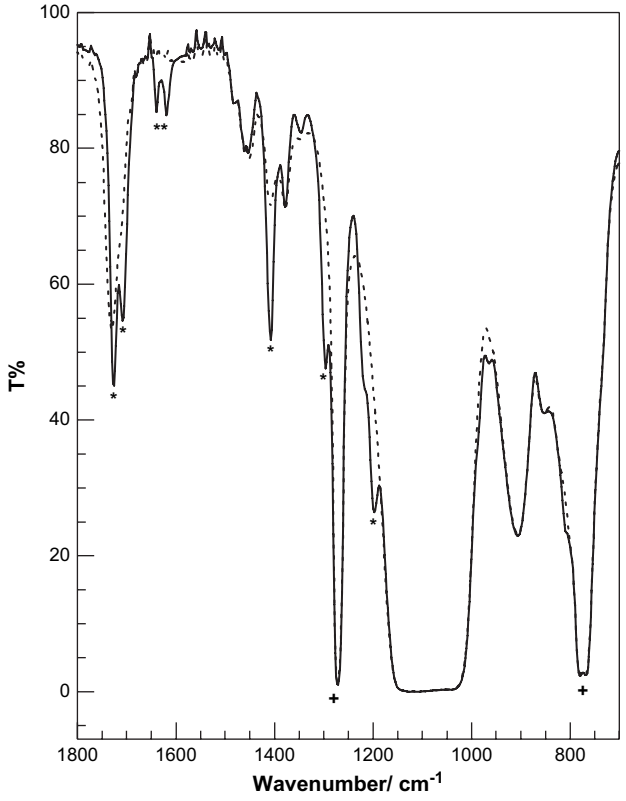

Fig. 5. FTIR spectra of a PMSSQ film containing PPO-TMPTA before (solid line) and after (dashed line) 193 nm exposure (total dose 3.0 J cm^{-2}, 12 mJ cm^{-2} $pulse^{-1}$, frequency 1.0 Hz). The spectrum for the exposed sample corresponds to the photobleaching end point. The "*" symbol on the solid line spectrum indicates absorption peaks corresponding to the acrylate and "+" to PMSSQ.

Analyzing the changes in Fig. 5 as a function of incident radiation dose in the region between 1800 and 1180 cm^{-1} is informative because: (i) the acrylate shows many characteristic bands: 1726 and 1708 cm^{-1} (C═O stretching), 1639 and 1619 cm^{-1} (C═C stretching), 1408 cm^{-1} (CH deformation), 1295 cm^{-1} (CH rock), and 1198 cm^{-1} (C–O stretch); (ii) PMSSQ is transparent in this region except for the characteristic sharp and strong peak at 1271 cm^{-1} ($Si–CH_3$ stretch); (iii) many bands are strongly affected by irradiation. Major changes in this region are the shape and position of the C═O stretch, centered at 1731 cm^{-1}, and the disappearance of acrylate bands at 1639, 1619, 1408, 1295 and 1198 cm^{-1}. Notably, no changes are observed in the intensity of the bands at 1271 cm^{-1} and at ~775 cm^{-1} ($SiCH_3$ Me rock, Si–C stretch) that are assigned to PMSSQ. The intense band between 1180 and 1000 cm^{-1} corresponds to the strong absorption of the Si–O stretch in PMSSQ [19,20] and to the C–O–C stretch for the ether units in PPO-TMPTA [17]. In summary, the FTIR data indicate that loss of acrylate C═C groups following 193 nm irradiation is the only significant chemical change.

3.7. NMR

Several thin films of PPO-TMPTA in PMSSQ were spin coated from a solution of PPO-TMPTA/PMSSQ 17:83 wt% in MEK on quartz disks at 1000 rpm in order to obtain thick films and then baked for 5 min at 90 °C. The UV–vis absorbance of the films was measured before and after successive 193 nm irradiations until the photobleaching end point was reached. The initial film absorbance at 193 nm was higher than 2.5 while the final was ~0.6. After reaching the end point, the films of irradiated sample were scrapped off from the quartz disk and dissolved in acetone-d_6, a good solvent for PPO-TMPTA and PMSSQ. The dissolution was incomplete, a gel-like sediment remaining in the tube. For comparison, a non-irradiated solution of PPO-TMPTA/PMSSQ in acetone-d_6 was prepared; its ^{1}H NMR spectrum is shown in Fig. 6 (top). Four groups of peaks are easily recognizable, three correspond to the acrylate, 6.4–5.9 ppm (olefinic CH), 3.8–3 ppm (OCH_2), and 1.4–0.8 ppm (alkyl H), and one for the PMSSQ − 0.8 ppm ($Si–CH_3$). The ^{1}H NMR spectrum for the irradiated sample is shown in Fig. 6 (middle). Compared to the non-irradiated sample, the peaks are rather broad and the peaks at ~6.4 to 5.9 ppm are weaker. The peak observed in the irradiated sample at 2.9 ppm is shifted to 3.7 ppm after addition of D_2O, Fig. 6 (bottom). The presence of D_2O also caused the disappearance of the broad band at ~5.7 ppm, making the decrease in the olefinic H peaks more evident. The ^{1}H NMR data indicate that the acrylate C═C bonds are consumed upon irradiation. The ^{13}C NMR spectrum for the non-irradiated sample shown in Fig. 6 (top)

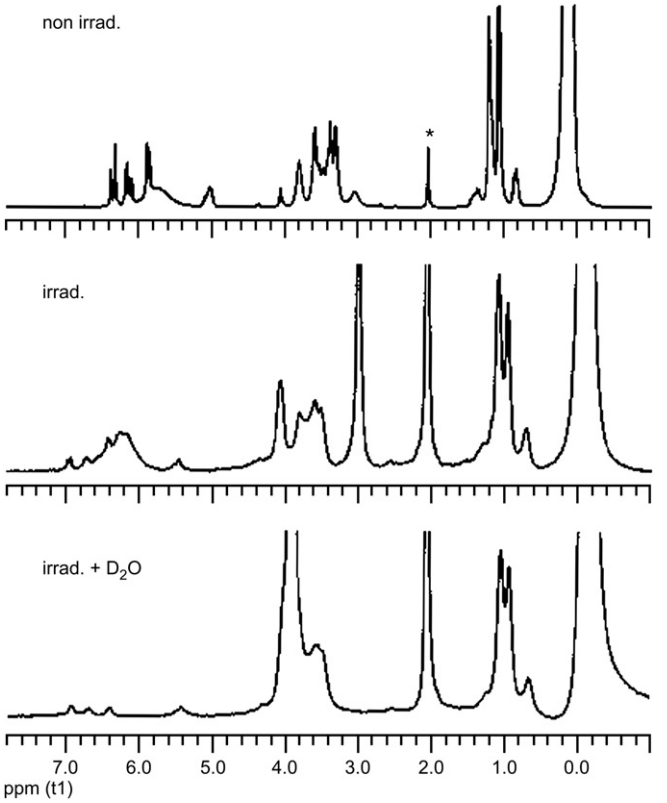

Fig. 6. The top trace corresponds to the ^{1}H NMR spectrum for a sample containing PPO-TMPTA and PMSSQ in acetone-d_6. The middle (without D_2O) and the bottom (with D_2O) traces correspond to a 193 nm irradiated film of PPO-TMPTA/PMSSQ that was dissolved in acetone-d_6.

and the following peaks, or groups, were assigned to the acrylate: 166 ppm (C═O), 130 ppm (C═C), 78–55 ppm (C–O), 44 ppm (C), 18 ppm (alkyl C); the broad peak at −3.2 ppm is assigned to Si–CH_3 from PMSSQ. Attempts to acquire the ^{13}C spectrum for the irradiated sample, using the same parameters used to acquire the spectrum for the non-irradiated samples, were unsuccessful. Since the parameters used were those commonly employed for small molecules in solution, this suggests that the formation of polymer has caused broadening of the ^{13}C signals. The formation of polymers is also supported by the broad peaks observed in the ^{1}H NMR spectrum and by the low solubility of the irradiated material in acetone-d_6. The partial ^{13}C spectrum of the irradiated sample was obtained in a 2D HMQC experiment [21], as shown in Fig. 7 (bottom), where only C with attached H can be observed. The resonance bands are broad and noticeably the resonance bands at ~130 ppm characteristic for C═C are absent, confirming loss of acrylate C═C bonds. The other peaks at 76–72, 57, 18–12, and 8 ppm are found also in the non-irradiated sample (Fig. 7, top) as well as the peak at −3.8 ppm. The NMR results, in agreement with the FTIR data, confirm loss of acrylate C═C bonds as the dominant chemical change.

3.8. Proposed mechanism

The goal of this work was to identify functional materials with good contrast enhancement properties for lithographic applications; further, new mechanistic information can guide the design of improved materials. In the absence, or even in the presence of photoinitiators, acrylates are directly excited when irradiated at 193 nm. Some aspects of the mechanisms proposed here are based on reported experimental and theoretical results on the direct photopolymerization of acrylates [7–9]. Important reactions to consider are shown in Scheme 2. When a photoinitiator was present, usually I-819, we assume that the photogenerated initiating radicals react following the generally accepted mechanism of photoinitiated polymerization of acrylates mediated by photoinitiators [22]. For direct

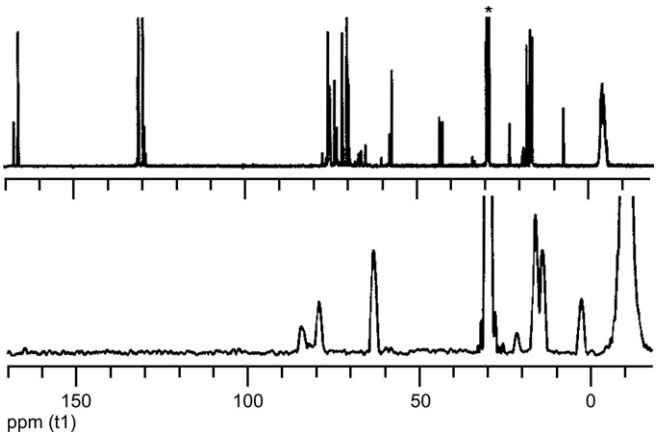

Fig. 7. The top trace corresponds to the ^{13}C NMR spectrum for a sample containing PPO-TMPTA and PMSSQ in acetone-d_6. The bottom trace corresponds to the ^{13}C NMR spectrum obtained from an HMQC experiment for a film of PPO-TMPTA/PMSSQ irradiated at 193 nm and dissolved in acetone-d_6.

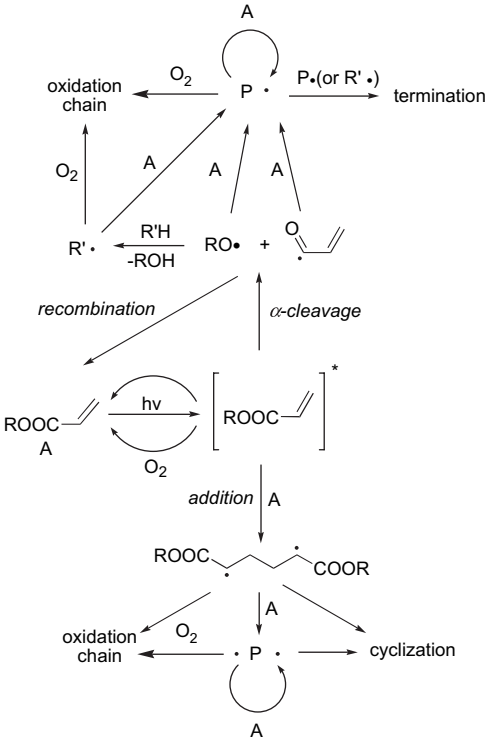

Scheme 2.

irradiation, explaining how radical centers can be generated is the key to mechanistic understanding.

Electron transmission and electron-energy loss spectroscopies suggest that the lower excited state of methyl acrylate and methyl methacrylate have $(\pi,\pi^*)^3$ character and is well separated from the higher (n,π^*) state [23]. This experimental observation is supported by recent computational work [24]. Thus, we expect that when acrylates are excited at 193 nm the triplet state will be formed following intersystem crossing (Scheme 2).

In some cases UV exposure does not lead to chemical change, e.g., triplet unimolecular decay mediated by C═C rotation or physical quenching by oxygen. The rotation decay path is common for α,β unsaturated carbonyl compounds and is the cause of their short triplet state lifetime [25]. Quenching by oxygen is common for triplets, the rate constants for α,β unsaturated carbonyls being around $2–5 \times 10^9\ M^{-1}\ s^{-1}$ in cyclohexane [25,26]. The process can be also effective in polymers, e.g., the quenching rate constant for 9-bromopyrene triplet in poly(dimethylsiloxane) (PDMS) films is $9.5 \times 10^9\ M^{-1}\ s^{-1}$ [27]. Given the similarities between PMSSQ and PDMS, similar triplet quenching rate constants by oxygen are anticipated.

Several reaction paths of triplet acrylates have been proposed by Knolle and Scherzer to explain the photopolymerization of acrylates by direct irradiation [8]. These processes have common elements with the photobleaching reported here. The paths proposed are based on transient data recorded for acrylates by laser flash photolysis in solution after direct irradiation (222 nm), as well as energy calculations performed using DFT B3LYP//6-31G(d) [7,8]. According to Knolle et al. the acrylate triplet state, highly localized at the vinyl group, can lead to inter- and intramolecular H-transfer to the

vinyl group as well as diradical formation. Both reactions are possible from an enthalpic point of view, but the latter is favored by about 15 kcal/mol and further substantiated by kinetic considerations. The relative importance of all the reaction channels depends on the surrounding matrix (solution or neat acrylate, structure and mobility of the side chain, etc.). They found that ether bonds in the acrylate backbone do not influence the primary reaction steps and that increasing the number of acrylate groups increases the rate of triplet dimerization (diradical) formation, probably the main reaction path in neat acrylates.

The same group reported formation of *n*-butanol by 222 nm direct photolysis of butyl acrylate in acetonitrile, with yields of *n*-butanol higher at low acrylate concentration ($<5 \times 10^{-4}$ M) [7]. Computational work suggests that direct α-cleavage (Scheme 2) of the acrylate triplet state to give butoxyl radicals is energetically unfavorable (+35.0 kcal/mol). However, the authors indicate that a probable explanation for the discrepancy between calculations and experiments may be that the cleavage can occur from a higher excited triplet state or solvent assisted cage reaction. The α-cleavage has been observed after multiphoton ionization (193 nm) in acrylate clusters in a molecular beam, where fragmentation with loss of EtO• in ethyl acrylate or MeO• in methyl acrylate occurs in a cationic acrylate cluster [28]. Below (see Scheme 3) we suggest an alternate route for the formation of alcohols in films.

In our system, the excited triplet acrylate can add to an acrylate, giving a diradical, or − less likely − can undergo α-cleavage to give alkoxyl and acroleinyl radicals (Scheme 2). Both reactions can lead to a net loss of at least one vinyl bond for each reactive event. The α-cleavage reaction has been included in the mechanism for completeness, since it has been proposed based on experiments in solution (*vide supra*); we favor the addition pathway. Acrylates quench the excited triplet acrylate in solution efficiently -7×10^8 M^{-1} s^{-1} for butyl acrylate and 2×10^9 M^{-1} s^{-1} for 1,4-butanediol diacrylate likely by addition [8]. The calculated energetics for the process are favorable, while hydrogen abstraction is unlikely for a π,π* excited state. In the films containing PPO-TMPTA, the more labile hydrogens are those in the $-CH_2O-$ in the PPO units. However, laser flash photolysis experiments involving diethyleneglycol diacrylate, carried out in solution, showed no evidence of a H abstraction by the triplet acrylate [7,8]. The efficiency of bimolecular reactions involving acrylate in the PMSSQ film, similar to the addition mechanism, will depend on its concentration. The concentration of acrylate units in a film of 10% PPO-TMPTA in PMSSQ is *ca.* 0.5 M, a concentration that should favor bimolecular processes.

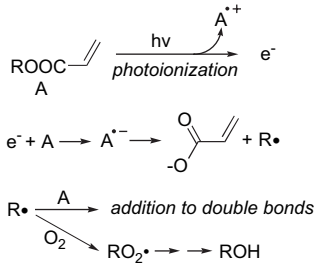

Scheme 3.

Molecular oxygen scavenges efficiently intermediates such as diradicals, radicals and triplet states. The deleterious effects of oxygen on the photopolymerization of acrylates in the presence of photoinitiators have been recognized and documented [22,29,30]. In addition, the reaction of triplet states and radicals with oxygen completely suppresses the direct photopolymerization reaction of a 1.2 μm layer of TMPTA in air under 222 nm irradiation from an excimer lamp (12 mW/cm^2) [9]. In contrast, in our case the effect of oxygen on the rate of photobleaching is limited. This may be caused by use of a pulsed laser. It has been reported that in the initiator mediated photopolymerization of acrylates, the inhibition period, due to oxygen presence in the acrylate, is shortened by replacing the UV lamp with a CW laser [31]. The shorter inhibition period results from higher intensity of the focused Ar laser (800×10^{-6} E cm^{-2} s^{-1}) compared to the medium pressure mercury lamp (1.5×10^{-6} E cm^{-2} s^{-1}) used. A similar result was reported for the ultrafast polymerization of acrylates by pulsed laser irradiation [32]. It was determined that during the induction period, under pulsed laser irradiation, each photoinitiator radical consumed one oxygen molecule; in contrast, 15 molecules were consumed with a conventional lamp. This probably results from the high peak power in the laser exposure, which prevents the development of the peroxidation chain reaction.

An approximate calculation of the number of photons delivered under our conditions and the oxygen content in the films can help to clarify the small effect of air on the photobleaching rate. In our experiments the energy is ≥2 mJ cm^{-2} pulse^{-1} (10 ns), which translates into 3.2 nmol of photons/cm^2/pulse (10 ns) = 0.32 E s^{-1} cm^{-2}. The moles of oxygen in 1 cm^2 of film are 0.3 nmol or less, considering that the oxygen concentration in silicones under air is ~3 mM [33], and that the film thickness is ≤1.0 μm. During the laser pulse, the diffusion of oxygen to the film is negligible, and thus the number of available photons exceeds the oxygen available. The small effect of oxygen on laser-induced acrylate photobleaching most likely results from its sacrificial depletion in the early stages of exposure. Diffusional processes that would normally restore the oxygen concentration are slow [34,35] for the pulse frequency used, and thus, most of the exposure occurs under essentially oxygen-free conditions.

Another possible mechanism for radical generation involves photoionization, where electron photoejection would lead to radical−cation formation. Further, electron capture by the acrylates would lead to fragmentation to form the acrylate carboxylate and an alkyl radical that can either add to double bonds or react with oxygen, ultimately leading to alcohol formation (Scheme 3).

4. Conclusion

The mechanism proposed involves reaction of excited acrylates to generate radical centers through addition to acrylates, photoionization, or less likely through α-cleavage. These processes lead to acrylate loss, as observed by FTIR and NMR.

The small oxygen effect on the efficiency of the process can be explained by its depletion via sacrificial reactions on the early stages of exposure. The radical species initially formed can add to other acrylates, just as they do in the propagation step in the polymerization of acrylates.

Beyond the proof-of-concept presented here, it is clear that practical challenges remain; thus for CEL applications one would need to identify casting solvents that do not interfere with those used for the resist layer. Further, the nature of the photobleaching processes identified would be entirely compatible with negative resists, but would require a delicate balance in the case of positive resists to ensure that the radical processes involved do not interfere with the requirements for efficient film solubilization during development.

The direct 193 nm irradiation of thin films containing the acrylate PPO-TMPTA in PMSSQ leads to an efficient photobleaching at that wavelength, with high contrast. The photobleaching reflects loss of the vinyl C=C groups, effectively converting π-bonds into σ-bonds. The acrylate PPO-TMPTA, which has a three-arm star-like structure with extended arms constituted by propoxy units with terminal acrylate moieties, was the most effective among several tested. This acrylate was also very compatible with the PMSSQ matrix, chosen because of its high transparency at 193 nm and its excellent film-forming properties. The effects of photoinitiators and plasticizers as film additives were also analyzed. The efficient photobleaching of thin films of acrylates in PMSSQ by direct 193 nm irradiation is an attractive option for contrast enhancement in photolithography at 193 nm.

Acknowledgments

This work was generously supported by grants from the Natural Sciences and Engineering Research Council of Canada and by Rohm and Haas (R&H). We thank Dr. B. Antrim (R&H) for conducting the AFM experiments, Dr. K. Willey (R&H) and G. Cuglietta for assistance with the laser exposure system, and Dr. G. Facey and C. McDonald for assistance with the NMR experiments.

References

[1] Drobny JG. Radiation technology for polymers. Boca Raton: CRC Press; 2003.
[2] Belfield KD, Crivello JV, editors. Photoinitiated polymerization. Washington, DC: American Chemical Society; 2003.
[3] Allcock HR, Lampe FW, Mark JE. Contemporary polymer chemistry. 3rd ed. Upper Saddle River: Prentice Hall; 2003.
[4] Medvedevskikh YG. Stationary and non-stationary kinetics of the photoinitiated polymerization. Zeist, Boston: VSP; 2004.
[5] Ebewele RO. Polymer science and technology. Boca Raton, London: CRC Press; 2000.
[6] Odian G. Principles of polymerization. Hoboken: Wiley Interscience; 2004.
[7] Knolle W, Scherzer T, Naumov S, Madani M. Coating 2004;37:416.
[8] Knolle W, Scherzer T, Naumov S, Mehnert R. Radiat Phys Chem 2003;67:341.
[9] Scherzer T. J Polym Sci Part A Polym Chem 2004;42:894.
[10] Crano JC, Guglielmetti RJ, editors. Organic photochromic and thermochromic compounds. New York: Plenum Press; 1999.
[11] Durr H, Bouas-Laurent H, editors. Photochromism: molecules and systems. Elsevier Science Ltd; 2003.
[12] Griffing BF. IIEE Electron Devices Lett 1983;1:14.
[13] Griffing BF, West PR. European Patent EP 0110165 B1; 1984.
[14] West PR, Davies GC. US Patent US 4663275; 1987.
[15] Gore R, Gallagher M, You Y. US Patent US 6903175 B2; 2005.
[16] (a) Srinivasan R, Braren B. Chem Rev 1989;89:1303;
(b) Sanrame CN, You Y, Scaiano JC. Unpublished results.
[17] Colthup NB, Daly LH, Wiberley SE. Introduction to infrared and Raman spectroscopy. 3rd ed. Boston: Academic Press; 1990.
[18] Jovanovic R, Dube MA. J Appl Polym Sci 2001;82:2958.
[19] Chua CT, Sarkar G, Chooi SYM, Chan L. J Mater Sci Lett 1999; 18:33.
[20] Chen C-H, Huang F-S. Thin Solid Films 2003;441:248.
[21] Friebolin H. Basic one- and two-dimensional NMR spectroscopy. 3rd ed. Weinheim: Wiley-VCH; 1998.
[22] Moad G, Salomon DH. The chemistry of free radical polymerization. 1st ed. Oxford: Pergamon, Elsevier; 1995.
[23] Schafer O, Allan M, Haselbach E, Davidson RS. Photochem Photobiol 1989;50:717.
[24] Garcia-Exposito E, Bearpark MJ, Ortuno RM, Robb MA, Branchadell V. J Org Chem 2002;67:6070.
[25] Bonneau R. J Am Chem Soc 1980;102:3816.
[26] Schuster DI, Dunn DA, Heibel GE, Brown PB, Rao JM, Woning J, et al. J Am Chem Soc 1991;113:6245.
[27] Chu DY, Thomas JK, Kuczynski J. Macromolecules 1988;21:2094.
[28] Morita H, Freitas JE, El-Sayed MA. J Phys Chem 1991;95:1664.
[29] Bhanu VA, Kishore K. Chem Rev 1991;91:99.
[30] Mueller U. J Macromol Sci Chem 1994;A31:1905.
[31] Decker C, Jenkins AD. Macromolecules 1985;18:1241.
[32] Decker C. J Polym Sci Polym Chem Ed 1983;21:2451.
[33] Ohyanagi M, Nishide H, Suenaga K, Tsuchida E. Polym Bull (Berlin) 1990;23:637.
[34] Masoumi Z, Stoeva V, Yekta A, Pang Z, Manners I, Winnik MA. Chem Phys Lett 1996;261:551.
[35] Yekta A, Masoumi Z, Winnik MA. Can J Chem 1995;73:2021.